

# THE EFFECT OF ROTATION ON A RAPIDLY SHEARED HOMOGENEOUS TURBULENT FLOW WITH A PASSIVE SCALAR

Geert Brethouwer  
 Department of Mechanics,  
 Royal Institute of Technology (KTH)  
 SE-100 44 Stockholm, Sweden  
 geert@mech.kth.se

## ABSTRACT

The effect of rotation on the time development of a homogeneous turbulent shear flow is studied by means of a series of direct numerical simulations. At the same time the influence of the rotation on the transport of a passive scalar in the turbulent shear flow is investigated. The shear rate used in this study is relatively high. The reason for this is that we want to approximate the situation in a turbulent boundary layer close to the wall. Because of the high shear rates the results of the numerical simulations can be compared with viscous rapid distortion theory based on the linearized equations of the flow and scalar fields. It is shown that rotation has a strong influence on the time development of the turbulent kinetic energy and anisotropy of the flow as well as on the direction of the turbulent scalar flux and on the scalar-velocity fluctuation correlation. Viscous rapid distortion theory predictions of the flow and scalar field agree in general well with the numerical simulations.

## INTRODUCTION

In atmospheric flows and oceans, and in many practical applications like gas turbines and cyclones rotation influences the turbulent flow field. As a consequence of its influence on turbulent flow, rotation also affects the turbulent transport of scalars like heat and contaminants. The most simple geometry with both shear and rotation is a homogeneous turbulent shear flow in a rotating frame. This particular geometry is of great interest for Reynolds-stress model (RSM) development but is also of fundamental importance. It has been studied by Bardina et al. (1983), Salhi & Cambon (1997) and Tanaka et al. (1998). Tanaka et al. studied the vortical structures at different rotation speeds by means of direct numerical simulations (DNS). Bardina et al. performed large-eddy simulations (LES) and studied the effect of rotation on development of the turbulent flow. Salhi & Cambon compared the LES of Bardina et al. with viscous rapid distortion theory (RDT) and found an overall reasonable agreement between the LES and RDT. The transport of scalars has only been studied in a non-rotating homogeneous turbulent shear flow to our knowledge (Rogers et al., 1989).

We present an analysis and DNS of homogeneous turbulent shear flow with a passive scalar field in a rotating frame. The shear rate is high and the scalar field has a linear and steady mean gradient. A series of DNS have been carried with a range of different rotation speeds. The results of the simulations are compared with viscous RDT. Our goal is to study the influence of rotation on the time development of the turbulent flow, similar to Bardina et al. (1983), but without a subgrid-model and with a much higher resolution

and a higher shear rate. The effect of rotation on turbulent transport of a passive scalar is investigated as well.

We now describe the details of the DNS and RDT and present some results on the time development of a homogeneous turbulent shear flow with a passive scalar field in a rotating frame.

## THE DIRECT NUMERICAL SIMULATIONS

The governing equations of the incompressible flow for a homogeneous turbulent shear flow in a rotating frame are

$$\nabla \cdot \mathbf{u} = 0 \quad (1)$$

$$\frac{\partial \mathbf{u}}{\partial t} + \mathbf{u} \cdot \nabla \mathbf{u} + Sx_3 \frac{\partial \mathbf{u}}{\partial x_1} + Su_3 \delta_{i1} + 2\boldsymbol{\Omega} \times \mathbf{u} = -\nabla p + \nu \nabla^2 \mathbf{u} \quad (2)$$

where  $\mathbf{u}$  is the fluctuating velocity,  $\nu$  the viscosity,  $S = \partial \bar{U}_1 / \partial x_3$  is the linear and constant mean velocity gradient and  $\boldsymbol{\Omega} = \Omega \mathbf{e}_2$  is the rotation vector where  $\mathbf{e}_2$  is the unit vector in the  $x_2$ -direction. The rotation speed of the frame is  $\Omega$ . The mean velocity profile, coordinate system and direction of rotation are sketched in figure 1. In the flow a passive

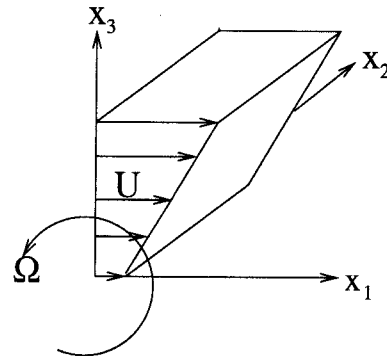


Figure 1: Sketch of the mean velocity profile, coordinate system and the direction of rotation.

scalar is present with a mean linear and constant scalar gradient  $\mathbf{G}$ . The transport equation for the fluctuation of the scalar  $\theta$  is given by

$$\frac{\partial \theta}{\partial t} + \mathbf{u} \cdot \nabla \theta + Sx_3 \frac{\partial \theta}{\partial x_1} + \mathbf{G} \cdot \mathbf{u} = \kappa \nabla^2 \theta \quad (3)$$

where  $\kappa$  is the diffusivity of the scalar. The term  $\mathbf{G} \cdot \mathbf{u}$  is a production term of scalar fluctuations.

The DNS of the three-dimensional turbulent flow and scalar mixing is carried out with a standard pseudo-spectral method. The size of the computational domain is  $4\pi \times 2\pi \times 4\pi$  with periodic boundary conditions in all three directions. The resolution of the DNS is  $320 \times 160 \times 320$ . The aliasing

errors are reduced by a combination of phase shifting and truncation. A fourth-order Runge-Kutta scheme is used for the time advancement. During the time advancement the coordinate system is moving with the mean flow field. It is remeshed with a regular time interval as in the computations of Rogers et al. (1989). Velocity and scalar fields are stored for post-processing when the coordinate system is non-skewed.

To obtain an initial velocity field a short DNS of decaying isotropic turbulence is carried out. The initial velocity field is approximately isotropic and has a Reynolds number of  $Re_\lambda = u'\lambda/\nu = 31.5$  where  $u'$  is the root mean square (rms) of the velocity fluctuations and  $\lambda$  the Taylor length scale. The initial integral turbulent length scale is 0.41 which gives a ratio of integral length scale to the box size in the  $x_1$  direction of 0.033. The initially isotropic field is then distorted by a constant and rapid shearing motion. The initial value of non-dimensional shear number  $SK/\varepsilon = 18$ , where  $K$  is the turbulent kinetic energy and  $\varepsilon$  the dissipation. This value is approximately the maximum value of the non-dimensional shear number in a turbulent channel flow (Moser et al., 1998) and turbulent boundary layer (Komminaho & Skote 2002) close to the wall.

Together with the flow the development of three passive scalars fields are simulated. The scalars have all a Schmidt/Prandtl number of  $\nu/\kappa = 0.7$  and have a mean scalar gradient in the  $x_1$ ,  $x_2$  and  $x_3$ -direction respectively. The evolution for any mean scalar gradient is then a simple superposition of these three passive scalar fields. The initial passive scalar fields are without scalar fluctuations but the mean gradient acts as a source of fluctuations.

### VISCOUS RAPID DISTORTION THEORY

The rapid distortion theory is based on the assumption that for a sheared flow the Navier-Stokes equations and the advection-diffusion equation for the scalars can be linearized. The assumption that the non-linear terms can be neglected is valid as long as the shear is rapid and the distortion time is not too long. For homogeneous flows the solution of the RDT equations for the flow and scalar field can be found in Fourier space. After elimination of the pressure the RDT equations in Fourier space are given by

$$\left(\frac{\partial}{\partial t^*} + \nu \frac{k^2}{S}\right) \hat{u}_i = \left(-\delta_{i1} + 2 \frac{k_i k_1}{k^2}\right) \hat{u}_3 + 2 \frac{\Omega}{S} \left(\epsilon_{ij2} - \frac{k_i k_n}{k^2} \epsilon_{nj2}\right) \hat{u}_j \quad (4)$$

$$\left(\frac{\partial}{\partial t^*} + \kappa \frac{k^2}{S}\right) \hat{\theta} = -\frac{G_i}{S} \hat{u}_i \quad (5)$$

with

$$\frac{dk_i}{dt^*} = -k_1 \delta_{i3} \quad (6)$$

where the time  $t^*$  is scaled with the shear rate and  $\epsilon_{ijk}$  is the permutation tensor. The viscous and diffusion terms are kept in the present analysis. To find the Reynolds stresses, scalar fluxes and other mean statistical moments the Fourier coefficients of the velocity and scalar have to be integrated in wave number space. However, then an energy spectrum is needed and a form for it has to be assumed. The statistical moments are independent of the form of the energy spectrum in case the viscosity is zero but then it is in fact assumed that  $SK/\varepsilon$  is infinite. Here it is assumed that the energy spectrum has the following form

$$E(k) = Ck^2 \exp(-2kl) \quad (7)$$

where  $k$  is the wave number,  $C$  a constant and  $l$  some characteristic turbulent length scale. The shape of this spectrum agrees fairly well with the DNS data. Using this spectrum it can be shown that

$$\frac{SK}{\varepsilon} = \frac{Sl^2}{6\nu} \quad (8)$$

The evolution of the statistical velocity moments according to the viscous RDT is now completely determined by the choice of  $Re^* = Sl^2/\nu$  and the rotation speed. Here  $Re^* = 108$  is taken which implies  $SK/\varepsilon = 18$  so that the initial value of the non-dimensional shear number of the DNS and viscous RDT are equal. The scalar spectrum is taken equal to the energy spectrum with the same value for the length scale  $l$ . All the statistical moments are computed by integrating the RDT equations in wave number space and time using numerical libraries.

### RESULTS OF THE SIMULATIONS AND RDT

Five cases have been simulated and analysed. All the simulations have the same initial isotropic turbulent flow field and shear rate but the rotation speed is varied. The following five cases have been considered:  $R = 2\Omega/S = 0$  (pure shear),  $R = -1/2$ ,  $R = -1$ ,  $R = -3/2$  and  $R = 1/2$ . We first study the time development of the flow field and then of the scalar field.

#### Flow field

The time development of the turbulent kinetic energy for the five cases is shown in figure 2. The symbols in this figure and the following figures represent the results of the DNS and the lines represent the results of the viscous RDT. Figure 2 shows that the time development of the energy at

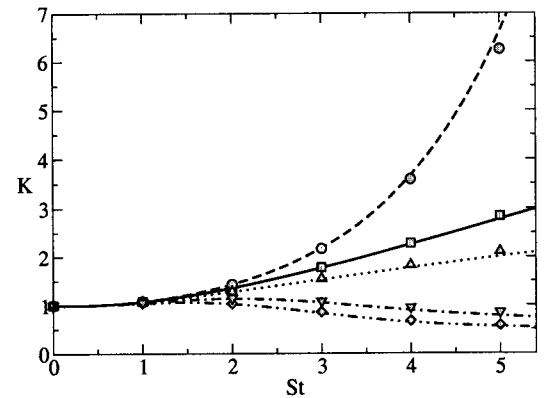


Figure 2: Time development of the turbulent kinetic energy  $K$  obtained from DNS (symbols) and RDT (lines). The time  $t$  is made non-dimensional with the shear rate  $S$  and the  $K$  is scaled with its initial value. ( $\nabla$ , - - - -),  $R = 1/2$ ; ( $\square$ , ———),  $R = 0$ ; ( $\circ$ , - - - -),  $R = -1/2$ ; ( $\triangle$ , ·····),  $R = -1$ ; ( $\diamond$ , - · - · - · -),  $R = -3/2$ .

different rotation speeds is very well predicted by the viscous RDT. A non-viscous RDT, which is not shown here, would overpredict the growth rate of the energy. The case  $R = -1/2$  is shown to be the most unstable case (Salhi & Cambon, 1997). Indeed, the energy grows very fast for  $R = -1/2$  and the flow is clearly destabilized by the rotation.

The energy grows much faster than in the case without rotation  $R = 0$  for example. For  $R = -1$  the energy still grows but for faster rotation speeds ( $R = -3/2$ ) the energy slowly decays and rotation is stabilizing the flow field. For positive  $\Omega$  ( $R = 1/2$ ) the flow is also stabilized by the rotation.

Figure 3 shows the development of the anisotropy of the turbulent fluctuations by means of one of the Reynolds stress components  $b_{11}$  where  $b_{ij} = \overline{u_i u_j} / (2K) - \delta_{ij} / 3$ . The

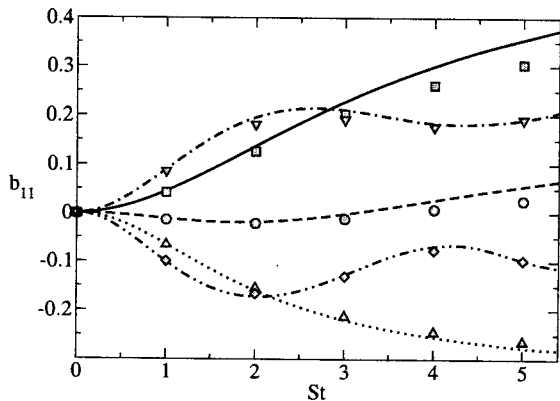


Figure 3: Time development of the Reynolds stress component  $b_{11}$ . Symbols and lines as in figure 2.

rotation clearly influences the anisotropy of the flow according to the simulations. When  $R = 0$  and  $R = 1/2$   $b_{11}$  is positive and the streamwise component of the velocity fluctuation is the largest component. In the most unstable case  $R = -1/2$  the velocity fluctuations in the three directions are approximately of the same magnitude. For faster negative rotation speeds ( $R = -1$  and  $R = -3/2$ ) the component in the  $x_3$ -direction is the largest fluctuating component. The anisotropy of the velocity fluctuations is quite well predicted by the viscous RDT. Only for large distortion times the anisotropy is sometimes slightly overpredicted, for instance for the non-rotating ( $R = 0$ ) case. The time development of the  $b_{13}$  component, which is related to the production of kinetic energy, is shown in figure 4. The most

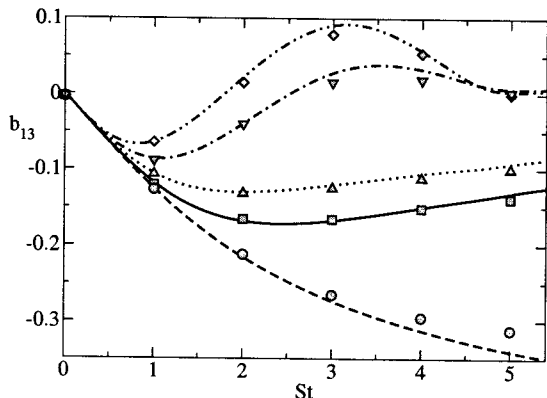


Figure 4: Time development of the Reynolds stress component  $b_{13}$ . Symbols and lines as in figure 2.

unstable case  $R = -1/2$  has the largest value for  $b_{13}$  and it is

still growing at  $St = 5$ . For  $R = 0$  and  $R = -1$ ,  $b_{13}$  reaches a maximum value after some time and then it slowly decays. For  $R = -3/2$  and  $R = 1/2$  the Reynolds stress component  $b_{13}$  becomes positive after some time which implies a negative production rate and a decrease of kinetic energy, but thereafter it returns to a value around zero. Viscous RDT predicts that in the stable cases  $R = -3/2$  and  $R = 1/2$  the Reynolds stress components  $b_{11}$  and  $b_{13}$  have an oscillatory behaviour (Salhi, 2002). The simulation time is however too short to be able to see these oscillations.

It is perhaps noteworthy to remark that according to linear analysis without the influence of pressure there is a symmetry between the cases  $R$  and  $-1 - R$ . However, the effect of pressure breaks this symmetry (Salhi & Cambon, 1997). Furthermore, the Reynolds stress equations show that without the influence of pressure the time development of  $\overline{u_1 u_1}$  at  $R$  is identical to the time development of  $\overline{u_3 u_3}$  at  $-1 - R$  and vice versa and the time development of  $\overline{u_1 u_3}$  is identical at  $R$  and  $-1 - R$ . In our case this implies that without pressure effects the cases  $R = -1$  and  $0$  and the cases  $R = -3/2$  and  $1/2$  should have the same time development for the energy and  $b_{13}$ . The DNS and viscous RDT show that this is not the case and therefore prove that the pressure has an important influence on the time development of the flow and its anisotropy.

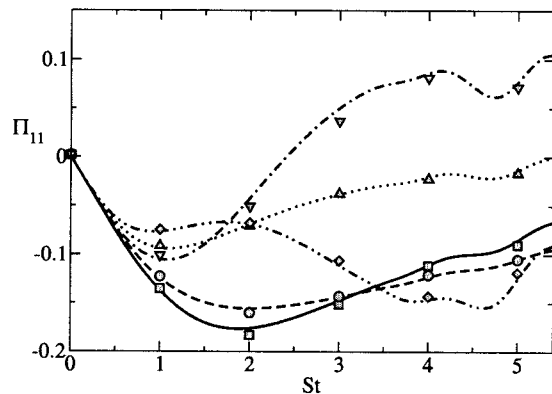


Figure 5: Time development of the rapid part of the pressure-strain correlation  $\Pi_{11}$ . Symbols and lines as in figure 2.

An important statistical moment for modeling is the pressure-strain correlation given by

$$\Pi_{ij} = p \left( \frac{\partial u_i}{\partial x_j} + \frac{\partial u_j}{\partial x_i} \right) \quad (9)$$

This pressure-strain correlation redistributes the energy between the different fluctuating velocity components. In general the pressure is split into a slow part related to non-linear processes and a rapid part related to the distortion of the flow. The rapid part of the pressure satisfies in our case

$$\nabla^2 p^{(r)} = (-2S - 2\Omega) \frac{\partial u_3}{\partial x_1} + 2\Omega \frac{\partial u_1}{\partial x_3} \quad (10)$$

In figure 5 the time development of the rapid part of the pressure-strain correlation  $\Pi_{11}$  scaled with  $SK$  is shown. The agreement between the viscous RDT and the DNS results is again good. The influence of the rotation on the redistribution of energy between the different fluctuating

velocity components is large. For  $R = 1/2$   $\Pi_{11}$  is even positive after approximately  $St = 2.5$  and adds therefore energy to the streamwise velocity component whereas in the other cases the rapid pressure-strain correlation redistributes the energy from the streamwise component to the other velocity components.

### Scalar field

We have seen that the turbulent flow is significantly influenced by the rotation of the system. Because of this alteration of the flow the turbulent transport of the scalars will also be affected by rotation. Here below we show some examples of this influence.

Figure 6 shows the time development of the ratio of the rms of the scalar fluctuation to the root mean square (rms) of the velocity fluctuations for the scalar with a mean gradient in the  $x_1$ -direction. Initially this ratio is zero because there are no scalar fluctuations at  $St = 0$ . Then the ratio grows very fast but levels off after some time. It seems to approach an asymptotic value for long distortion times except in the case  $R = 0$  and  $R = 1/2$  where a decrease of the growth rate not yet can be observed at  $St = 5$ . In these cases the ratio of the scalar fluctuations and the velocity fluctuations grows significantly faster than in the cases with a negative rotation speed. The rotation has also an effect on the rela-

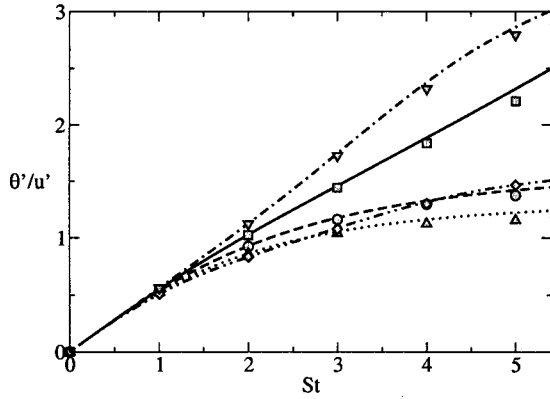


Figure 6: Time development of  $(\theta'/G)/(u'/S)$  for  $G = Ge_1$ . Symbols and lines as in figure 2.

tive intensity of the scalar fluctuations for the scalar with a mean gradient in the  $x_2$ -direction as can be seen in figure 7. For the scalar with a mean gradient in the  $x_3$ -direction the rotation has more or less the opposite effect as for the scalar with a mean gradient in the  $x_1$ -direction. The ratio of the scalar fluctuations to the velocity fluctuations grows faster for the cases with a high negative rotation speed ( $R = -1$  and  $R = -3/2$ ) as shown in figure 8. Moreover, we see that the viscous RDT gives an accurate description of the growth of the scalar fluctuations.

Figure 9 shows the scalar flux coefficient  $\overline{u_1\theta}/u_1'\theta'$  for the scalar with a mean gradient in the  $x_1$ -direction. In the non-rotating case ( $R = 0$ ) and in the most unstable case ( $R = -1/2$ ) the scalar flux coefficient is large and its value is around -0.9. In the other cases the coefficient decreases faster during the distortion. Especially in the case  $R = -3/2$  the scalar-velocity coefficient has a small value, approximately -0.3. Scalar-velocity fluctuation correlations are thus significantly affected by system rotation. This can

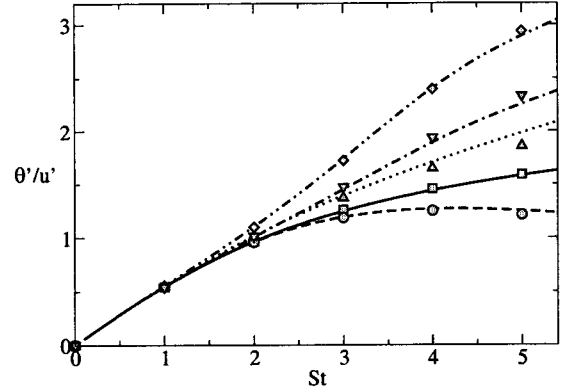


Figure 7: Time development of  $(\theta'/G)/(u'/S)$  for  $G = Ge_2$ . Symbols and lines as in figure 2.

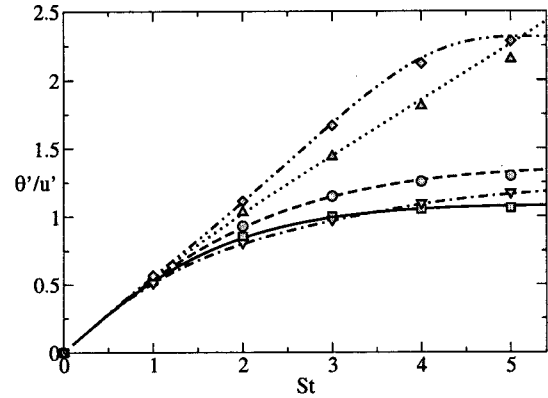


Figure 8: Time development of  $(\theta'/G)/(u'/S)$  for  $G = Ge_3$ . Symbols and lines as in figure 2.

also be observed in figure 11 which presents the scalar flux coefficient  $\overline{u_3\theta}/u_3'\theta'$  for the scalar with a mean gradient in the  $x_3$ -direction. In the cases  $R = 1/2$  and  $R = -3/2$  the scalar coefficient is much smaller than in the other cases. The viscous RDT does not give a very accurate prediction of the time development of the scalar flux coefficient for all cases but it gives nevertheless a correct answer on the question whether rotation reduces or enhances the scalar-velocity correlation.

For the scalar with a mean gradient in the  $x_2$ -direction the rotation has a less strong influence on the scalar flux coefficient as can be seen in figure 10 but the effect is still significant. In the cases that rotation is stabilizing the turbulent flow ( $R = 1/2$  and  $R = -3/2$ ) the scalar flux coefficient is smaller than in the other cases.

We have seen that rotation affects the scalar-velocity fluctuation correlation. We now study the effect of rotation on the direction of the turbulent scalar flux. It is well known that in turbulent shear flows the direction of the turbulent scalar flux and the mean scalar gradient do not coincide (Rogers et al., 1989). Figure 12 shows the time development of the angle  $\alpha$  of the turbulent scalar flux vector defined as

$$\alpha = \tan^{-1}(\overline{u_3\theta}/\overline{u_1\theta}) \quad (11)$$

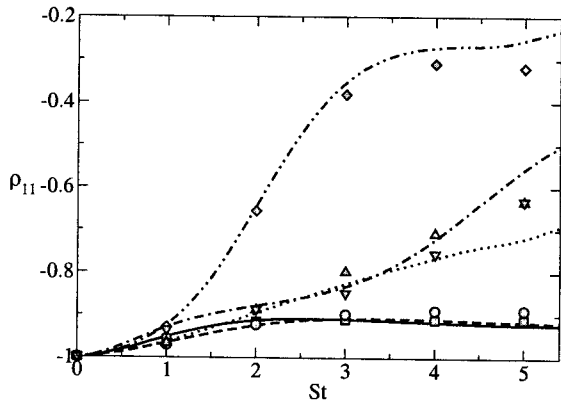


Figure 9: Time development of the scalar flux coefficient  $\overline{u_1\theta}/u_1'\theta'$  for  $G = Ge_1$ . Symbols and lines as in figure 2.

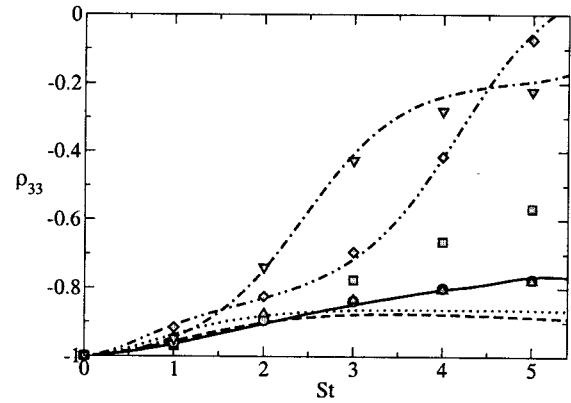


Figure 11: Time development of the scalar flux coefficient  $\overline{u_3\theta}/u_3'\theta'$  for  $G = Ge_3$ . Symbols and lines as in figure 2.

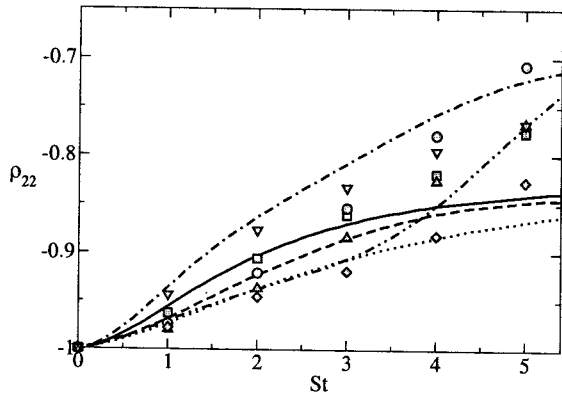


Figure 10: Time development of the scalar flux coefficient  $\overline{u_2\theta}/u_2'\theta'$  for  $G = Ge_2$ . Symbols and lines as in figure 2.

for the scalar with a mean gradient in the  $x_1$ -direction. This  $\alpha$  is in fact the angle between the direction of the turbulent scalar flux and the  $x_1$ -axis. Note that for the scalar with a mean gradient in the  $x_1$ -direction  $\alpha = 0^\circ$  implies that the direction of the turbulent scalar flux is aligned with the mean scalar gradient. The shear and the additional effect of system rotation results in a large variation of the direction of the scalar flux vector. For large negative rotation speeds the angle between the scalar flux vector and the mean scalar gradient is very large. In the case  $R = -1$  for example at  $St = 5$  the component of the scalar flux vector in the cross-stream direction is significantly larger than the component in the streamwise direction. Furthermore, observe that  $\alpha$  is well predicted by the viscous RDT. Figure 13 shows the time development of the angle  $\alpha$  for different rotation speeds but now for the scalar with a mean gradient in the  $x_3$  direction. For  $R = -1$   $\alpha$  is close to  $-90^\circ$  which implies that the scalar flux vector almost is aligned with the mean scalar gradient in the  $x_3$ -direction. At  $R = 1/2$ ,  $R = 0$  and  $R = -1/2$  on the other hand the scalar flux vector has a large component in the  $x_1$  direction. The case  $R = -3/2$  has also a large scalar flux component parallel to the  $x_1$ -axis but the scalar flux points approximately in the opposite direction compared to the case  $R = 0$ . All these trends are well described by the

viscous RDT.

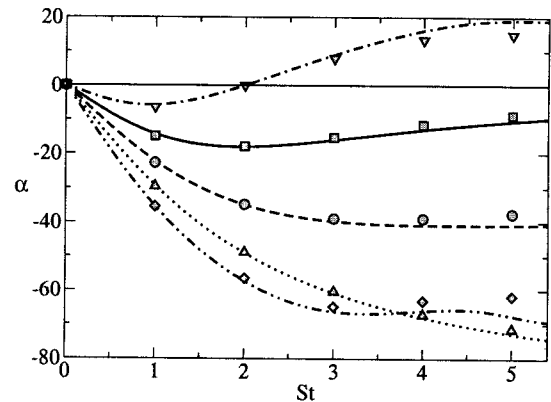


Figure 12: Time development of the angle  $\alpha = \tan^{-1}(\overline{u_3\theta}/\overline{u_1\theta})$  for  $G = Ge_1$ . Symbols and lines as in figure 2.

## CONCLUSIONS

The time development of a rapidly sheared homogeneous turbulent flow in a rotating frame has been studied by means of direct numerical simulations. In this geometry also the turbulent transport of a passive scalar with a mean gradient is investigated in order to study the effect of rotation on mixing. The results of the DNS have been compared with viscous rapid distortion theory. We come to the following conclusions.

- The structure of a turbulent flow field and passive scalar field change drastically and in a short time scale when it is distorted by a rapid shearing motion and a fast rotation of the system.
- The rotation speed of the system has a significant influence on the growth of the kinetic energy, anisotropy, pressure-strain correlations of a sheared turbulent flow.
- Rotation has also a large influence on passive scalar mixing in a turbulent flow. It affects the intensity of

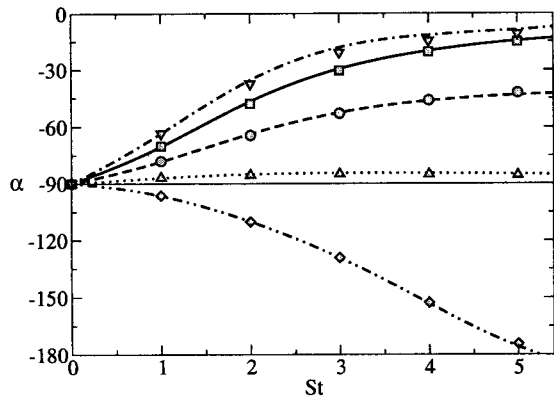


Figure 13: Time development of the angle  $\alpha = \tan^{-1}(\overline{u_3\theta}/\overline{u_1\theta})$  for  $G = Ge_3$ . Symbols and lines as in figure 2.

the scalar fluctuations and the scalar-velocity fluctuation correlations. Furthermore, rotation significantly affects the direction of the turbulent scalar flux. The flux is in general not aligned with the mean scalar gradient.

- Comparison between DNS and RDT shows that viscous RDT in general gives a good prediction of the one-point statistics of the turbulent velocity and scalar field for short distortion times. It seems therefore attractive to make RSM consistent with RDT for short distortion times.

#### ACKNOWLEDGEMENTS

The author wishes to thank Anshu Dubey and the Astronomy & Astrophysics department of the University of Chicago for making their numerical code available, and Arne Johansson for the valuable discussions.

#### REFERENCES

- Bardina, J., Ferziger, J.H., Reynolds, W.C. 1983 Improved turbulence models based on large-eddy simulation of homogeneous incompressible turbulent flow. *Tech. Rep. TF-19*. Stanford University.
- Komminaho, J., Skote, M. 2002 Reynolds stress budgets in Couette and boundary layer flows. *Flow, Turbul. Combust.* **68** pp. 167–192.
- Moser, R.D., Kim, J., Mansour, N.N. 1999 Direct numerical simulation of turbulent channel flow up to  $Re_\tau = 590$ . *Phys. Fluids* **11**, pp. 943–945.
- Rogers, M.M., Mansour, N.N., Reynolds, W.C. 1989 An algebraic model for the turbulent flux of a passive scalar. *J. Fluid Mech.* **203**, pp. 77–101.
- Salhi, A. 2002 Similarities between rotation and stratification effects on homogeneous shear flow. *Theoret. Comput. Fluid Dynamics* **15**, pp. 339–358.
- Salhi, A., Cambon, C. 1997 An analysis of rotating shear flow using linear theory and DNS and LES results. *J. Fluid Mech.* **347**, pp. 171–195.
- Tanaka, M., Yanase, S., Kida, S., Kawahara, G. 1998 Vortical structures in rotating uniformly sheared turbulence. *Flow, Turbul. Combust.* **60** pp. 301–332.